# Investigation of the Nanocellular Foaming of Polystyrene in Supercritical $CO_2$ by Adding a $CO_2$-Philic Perfluorinated Block Copolymer

**Jose Antonio Reglero Ruiz,[1,2] Eric Cloutet,[1,2] Michel Dumon[1,2]**

[1]*Université de Bordeaux, Laboratoire de Chimie de Polymères Organiques (LCPO), IPB/ENSCBP, 16 Avenue Pey-Berland, 33607 Pessac, Cedex, France*
[2]*Centre National de la Recherche Scientifique, CNRS, Laboratoire de Chimie de Polymères Organiques, IPB/ENSCBP, 16 Avenue Pey-Berland, 33607 Pessac, Cedex, France*

Received 10 September 2011; accepted 8 November 2011
DOI 10.1002/app.36455
Published online in Wiley Online Library (wileyonlinelibrary.com).

**ABSTRACT:** Nanocellular foaming of polystyrene (PS) and a polystyrene copolymer (PS-*b*-PFDA) with fluorinated block (1,1,2,2-tetrahydroperfluorodecyl acrylate block, PFDA) was studied in supercritical $CO_2$ ($scCO_2$) via a one-step foaming batch process. Atom Transfer Radical Polymerization (ATRP) was used to synthesize all the polymers. Neat PS and PS-*b*-PFDA copolymer samples were produced by extrusion and solid thick plaques were shaped in a hot-press, and then subsequently foamed in a single-step foaming process using $scCO_2$ to analyze the effect of the addition of the fluorinated block copolymer in the foaming behaviour of neat PS. Samples were saturated under high pressures of $CO_2$ (30 MPa) at low temperatures (e.g., 0°C) followed by a depressurization at a rate of 5 MPa/min. Foamed materials of neat PS and PS-*b*-PFDA copolymer were produced in the same conditions showing that the presence of high $CO_2$-philic perfluoro blocks, in the form of submicrometric separated domains in the PS matrix, acts as nucleating agents during the foaming process. The preponderance of the fluorinated blocks in the foaming behavior is evidenced, leading to PS-*b*-PFDA nanocellular foams with cell sizes in the order of 100 nm, and bulk densities about 0.7 $g/cm^3$. The use of fluorinated blocks improve drastically the foam morphology, leading to ultramicro cellular and possibly nanocellular foams with a great homogeneity of the porous structure directly related to the dispersion of highly $CO_2$-philic fluorinated blocks in the PS matrix. © 2012 Wiley Periodicals, Inc. J Appl Polym Sci 000: 000–000, 2012

**Key words:** ATRP; fluoro acrylate; polystyrene block copolymers; nanocellular foams; supercritical carbon dioxide

## INTRODUCTION

In the last years, the use of supercritical carbon dioxide ($scCO_2$) as a medium for polymer synthesis and for polymer processing has increased greatly.[1–3] The unique properties associated with supercritical fluids, and especially with $scCO_2$, due to its chemical, environmental, and economical advantages, have been explored for a long time in fields such as organic synthesis, catalysis, and materials science. Another investigation line is focused on the production of micro and nano of cellular materials using $scCO_2$ as a physical foaming agent, and in our case, directing the foams towards micro/nano bulk polymer foams. Nano polymer foams can be considered as foams which average cell size is below 100 nm while micro cellular polymer foams have a cell size between ca 0.1 and 10 μm.

*Correspondence to:* J. Antonio R. Ruiz (jareglero@gmail.com).




The gas foaming process takes place in several steps. In the first step, the polymer is saturated with $CO_2$ in the supercritical regime (above 7 MPa and 30°C), during a fixed time to reach the polymer-$scCO_2$ equilibrium swelling state.[4–8] After saturation, the sample, approaching or being in a rubbery state, is depressurized to atmospheric pressure to allow the gas expansion, taking advantage of the swelling and plasticization of the polymer, which reduces the glass transition temperature. In this method, the micro cellular structure may be controlled by changing the saturation temperature and the depressurization rates.

In the range of micro cellular foams, several porous amorphous polymers such as polystyrene, polycarbonate or semicrystalline polymers (polyethylene, polypropylene) have been obtained[9–12] via a $scCO_2$ process.

Conversely, the solubility of $CO_2$ in different polymers has been studied.[8,13–15] Solubility or $CO_2$ philicity is closely related to polymer swelling. Polymers have in general a limited solubility in supercritical fluids (SF) and e.g., in $scCO_2$. However $scCO_2$ often allows depressing significantly the glass

transition temperature ($T_g$) of several amorphous polymers. This plasticization effect is a key parameter to control the foaming process of amorphous polymers and therefore the main structural characteristics of the materials obtained, as it has been previously mentioned by different authors.[16–19] Indeed it is well known that fluorinated or siloxane polymers present the highest $CO_2$ – phicility,[20–23] higher than classical polymers such as polystyrene, polycarbonate or polymethyl(methacrylate). Following this strategy, block (co)polymers have been used as surfactants in dispersion heterogeneous polymerization of styrene or methacrylate monomers in $scCO_2$.

The syntheses of diblocks were carried out by means of sequential controlled radical polymerization techniques (RAFT reversible addition fragmentation chain transfer or NMP nitroxide-mediated polymerization) to produce copolymers formed mostly by a polystyrene block and a perfluorinated acrylate block, namely 1,1-dihydroperfluorooctylacrylate PFOA, or 1,1,2,2-dihydroperfluorodecylacrylate PFDA[24,25] (or sometimes a polyethylene oxide block). Furthermore these copolymers are shown to self assemble in $scCO_2$ into core shell structures or micelles.[26] We can cite the synthesis of polyurethane in $ScCO_2$ using PDMS as reactive stabilizer.[27]

In the last years, some work has been carried out to obtain nanocellular porous structures using block copolymers with highly $CO_2$ philic blocks, especially fluorinated blocks or methacrylate blocks and $CO_2$ as blowing agent.[20–25] But only thin films were analyzed, neither polymer blends were considered. Besides the polymers under investigation resulted from a difficult synthesis.

In this work, we follow a line of investigation on submicron porous polymers with a relatively easy synthetic route, namely ATRP (Atom Transfer Radical Polymerization).[28–31] The comparative foaming of rather thick pieces of both neat PS polymer and PS-*b*-PFDA diblock copolymers is carried out.

The main objective is to analyze the influence of the fluorinated separated blocks in a PS matrix and to estimate the possible use of these fluorinated blocks as nucleating sites for $scCO_2$ bulk foaming of thick polymer parts. Structuration of copolymers into nanostructured blends was demonstrated to be efficient towards producing submicron cellular polymers.[32,33] Finally because $CO_2$ absorption increases with decreasing temperature[34] and entering a glassy state is favorable to nano or sub micro foaming, we intend to incorporate $CO_2$ at a low temperature (e.g., 0°C). Therefore the expected mechanism is the foaming of highly $CO_2$-philic fluoropolymer nuclei (issued from nano structuration of perfluoro copolymers) in a rigid glassy PS matrix in order to limitate the growth of the cells.

## EXPERIMENTAL

### Materials

The styrene monomer (Aldrich, >99%) was used after distillation over $CaH_2$. 1H,1H,2H,2H-perfluorodecyl acrylate (i.e., 1,1,2,2-tetrahydroperfluorodecyl, FDA, Aldrich), was distilled under reduced pressure and passed through a column of neutral alumina to remove inhibitor. In addition, for the polystyrene polymerization, 2,2′-bipyridine (Aldrich, 99%), 1-bromoethylbenzene (Aldrich, 99%) and copper bromide CuBr(I) (Aldrich) were used as received.

Cyclohexanone (Aldrich) was distilled over sodium sulphate and used as a solvent, whereas tetrahydrofuran (THF, Aldrich, 99%) was used for purification. Methanol (Aldrich, 99%) and Pentane (Aldrich, 99%) were used as received.

1,1,4,7,10,10-hexamethyltriethylenetetramine (HMTETA, Aldrich, 97%) and Ethyl-α-bromoisobutyrate (Aldrich, 99%) were used as received. In this case, tetrahydrofuran (THF) and α,α,α-trifluorotoluene (Aldrich, 99%) were used as received for solubilization and purification of the PS-*b*-PFDA copolymer.

### Polymerization

The synthesis of PS by ATRP was adapted from previous procedures[35,36] using bromo ethylbenzene as initiator in combination with CuBr/bipyridine (CuBr/bpy). The resulting polystyrene was used as a macroinitiator for the growth of the perfluorinated block.

In a similar way, the synthesis of PS-*b*-PFDA by ATRP was adapted from a previous procedure[36] using bromo ethylbenzene as initiator in combination with CuBr/1,1,4,7,10,10-hexamethyltriethylene tetramine (CuBr/HMTETA) as a catalytic system.

a. Synthesis of polystyrene ω-terminated with a secondary bromide (ω-Br-Ps).
   A Schlenk flask equipped with a magnetic stirrer bar is charged with 0.4 g (2.16 mmol) of 1-bromoethyl benzene, 0.31 g (2.16 mmol) of Cu(I)Br, 1.35 g (8.64 mmol) of bypiridine and 11.8 mL (104 mmol) of styrene. After three freeze-vacuum-thaw cycles to degas the system, the flask is then filled with argon and placed in a oil bath at 130°C and kept under stirring at 400 rpm during 1 h; the targeted theoretical molar mass is:

$$M_{\text{theo}} = \frac{m_{\text{monomer}}}{n_{\text{initiator}}} = \frac{11.8 \times \rho_{\text{styrene}}}{2.16 \times 10^{-3}} \approx 5000 \text{ g/mol} \quad (1)$$

   The resulting polymer was dissolved in THF and filtered over a column of neutral alumina to remove the copper species. Then the final

polymer was precipitated in methanol. The recovered powder was dried under vacuum at room temperature and collected in very high yield (90%).

b. Synthesis of poly(styrene) -*b*-poly(1H,1H,2H, 2H-perfluorodecyl acrylate) block copolymer.
A Schlenk flask equipped with a magnetic stirrer bar was charged with 0.2654 g (1.85 mmol) of Cu(I)Br, 0.4262 g (1.85 mmol) of HMTETA, 4 mL of cyclohexanone and 0.3914 g (1.85 mmol) of ethyl-α-bromoisobutyrate, used as initiator, with the molar ratio of Cu(I)Br:HMTETA:bromoisobutyrate = 1 : 1 : 1. After adding the require quantities of PS and FDA (i.e., 5.5 g and 9.6 g, respectively), corresponding to $18.5 \times 10^{-3}$ mol, in the case of a targeted molar mass of approximately 5400 g/mol for the PFDA block, the solution was submitted to three freeze-vacuum-thaw cycles to degas the system. Then the flask is filled with argon and placed in a oil bath at 120°C and kept under stirring at 400 rpm during 12 h. The viscous mixture was cooled down overnight, diluted in α,α,α-trifluorotoluene and passed through a column of neutral alumina to remove remaining catalyst. After evaporation of the solvent, the resulting polymer was washed twice in pentane. The recovered powder was dried under vacuum at room temperature and collected in high yield (90%).

### Chemical and thermal characterization of polymers

Chemical structure of the polymers was determined by using $^1$H-NMR. A Bruker Avance 400 MHz NMR spectrometer was employed, in $^1$H mode, at room temperature. Chemical shifts refer to tetramethylsilane as a reference. Deuterated benzene $C_6D_6$ was used as a solvent, whereas for the fluoro copolymers, hexafluoroisopropanol-d (HFIP-d) was employed.

The number average molar masses ($\overline{M}_n$) and dispersity index ($D = \overline{M}_w/\overline{M}_n$) were determined by size exclusion chromatography in a PL-GPC50Plus device using THF (tetrahydrofuran) as a solvent with a concentration of 3 mg/mL with UV detection at 254 nm. Finally, glass transition temperature ($T_g$), were measured in a DSC equipment, using a heating cycle from −150°C to 200°C at 5°C/min.

### Bulk sample preparation

Solid thin films were prepared by hot-pressing, with a pressure and temperature control. For a complete densification of the polymer powder, pressures of 14 MPa and temperatures up to 80°C were employed, during a fixed time of 5 min. Samples obtained (20 × 10 mm$^2$) showed a good surface appearance, with a regular thickness of 200 μm; no voids or empty zones were detected optically. Three specimens of each polymer, neat PS and PS-*b*-PFDA polymers were produced.

Density of the samples was between 0.98 g/cm$^3$ and 1.02 g/cm$^3$ in all cases, using the Archimedes principle. These density values show a rather good densification process to produce solid specimens that will be employed in the supercritical foaming process.

### Supercritical $CO_2$ foaming

$ScCO_2$ saturation and foaming is operated in a single-step batch process. The experiments were carried out in a high pressure reactor provided by Top Industrie (France), with a capacity of 300 cm$^3$ and capable of operating at maximum temperature of 250°C and maximum pressure of 40 MPa. The reactor is equipped with an accurate pressure pump controller provided by Teledyne ISCO, and controlled automatically to keep the temperature and pressure at the desired values with a precision of 0.1°C and 0.01 MPa, respectively.

$CO_2$ saturation pressure was fixed at 30 MPa for all the experiments, with a saturation temperature of 0°C during 16 h (the vessel was immersed in an ice bath prior to and during the foaming process). Foaming was carried out in a single step process, using a depressurization rate of 5 MPa/min. The $CO_2$ vessel temperature and pressure were monitored in the course of the process. The reported temperature values give a rough idea of the sample temperature during the foaming process because the observed temperature drop is dependent on the vessel volume and on the pressure drop rate, so that the measured temperature does not represent the real sample temperature due to poor thermal conductivity of polymers. However the temperature vs. time plots can be used to evaluate the vitrification delay of the samples. In Figure 1 is presented the temperature–pressure evolution during the foaming process, showing a decrease of the sample temperature inside the reactor down to −70°C, due to the depressurization.

### Foam density

Bulk foam density $\rho_f$ was determined by water-displacement method, based on Archimedes principle. Densities were calculated by measuring the volume of water displaced by the sample divided by the sample mass. At least three measurements were carried out for each sample produced.

### SEM observations

The cellular structure was analyzed by means of Scanning Electron Microscopy (SEM HITACHI S-

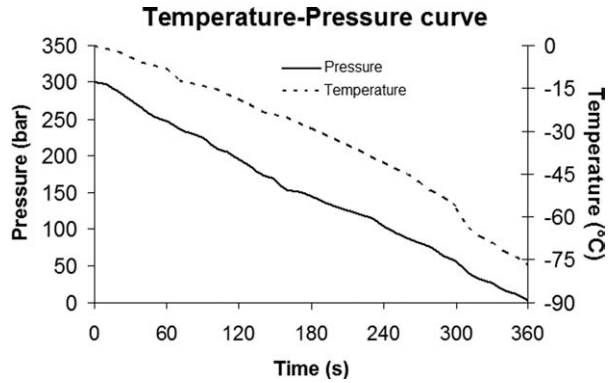


**Figure 1** Temperature and pressure evolution measured during a foaming process at a depressurization rate of 50 bar/min.

3000N). For the preparation of the samples, foams were frozen in liquid nitrogen and fractured to assure that the microstructure remained intact. For the observations, surfaces were coated with gold using a sputter coater (model EMSCOPE SC 500), in argon atmosphere. Cell size $\phi$ was obtained from direct observation from SEM micrographs, using a minimum of 100 cells in each calculation; whereas number cell density, here the average number of cells/volume unit, $N_C$ (cells/cm$^3$) was estimated from the following equation,[37] where $\rho_f$ and $\rho_s$ are the foam and solid material density, respectively:

$$N_C \cong 10^3 \frac{6\left[1 - \left(\rho_f / \rho_s\right)\right]}{\pi\phi^3} \quad (2)$$

## RESULTS

### Polymer characterization

The average molar mass, $\overline{M}_n$, of the PS block, determined by size exclusion chromatography (as a macroinitiator before the second block growth) is about 5400 g/mol and dispersity index $D \cong 1.4$. The average molar mass of the PS-*b*-PFDA copolymer is

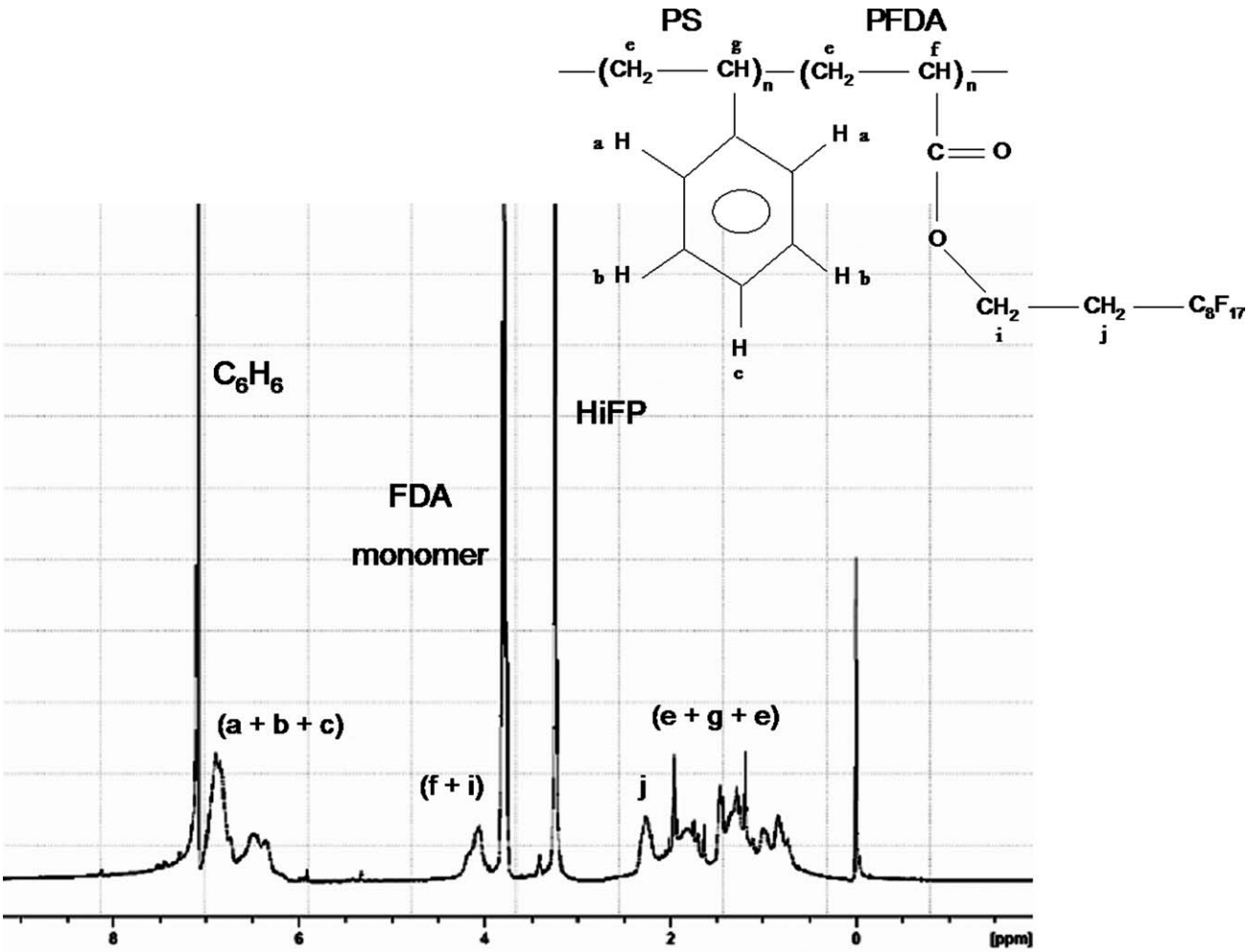


**Figure 2** PS-*b*-PFDA $^1$H-NMR spectra in a solvent mixture of benzene $C_6D_6$ and deuterated hexafluoroisopropanol (HFIP-d).

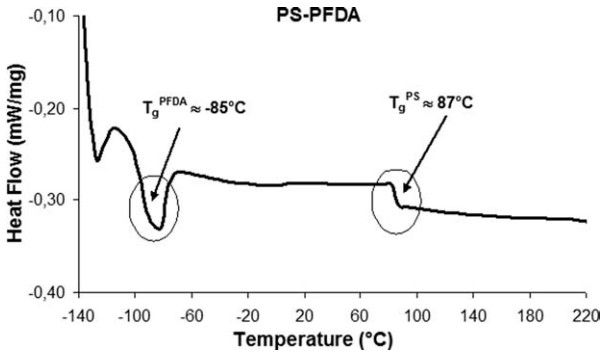


**Figure 3** DSC thermogram of the PS-*b*-PFDA copolymer.

9800 g/mol, providing blocks of 5400 g/mol and 4800 g/mol respectively with a final dispersity index $D \cong 1.5$.

The chemical structure of the copolymer is confirmed by $^1$H-NMR (Fig. 2), it contains a small fraction of FDA residual monomer, which does not inhibit its use in blends or the bulk neat samples. The relative area of the peaks indicates a relative percentage of each block about 60% for the PS block and 40% for the PFDA block.

The second scan of the DSC thermogram of the copolymer is presented in Figure 3 and reveals two $T_g$ : PS at 87°C and PFDA at −85°C. A $T_g$ was detected with difficulty at very low temperature. Although this $T_g$ step exhibits an unusual shape (due to the difficulty of base line stabilization), it is attributed to the PFDA block. However, the neat homopolymer PFDA is cited to have a crystalline behavior at long chain length.[30] Here, the chains are much shorter.

### Morphology of polymers (before foaming)

Scanning electron microscopy (SEM) observations were carried out on solid samples to characterize the morphology of both polymers. In Figure 4 are presented two SEM micrographs of the PS-*b*-PFDA block copolymer in bulk, showing a regular structure in which the fluorinated blocks are nanospheres embedded in the PS matrix. Considering that the composition of the copolymers is about 60% PS and 40% PFDA, this observed structure could be unusual but was already observed in micelle forms.[38,39] We believe that the morphology of bulk samples could be affected by the fabrication process, in our case the hot-pressing. On the other hand, Figure 5 shows two SEM micrographs of the neat PS, in which a typical homogeneous one-phase structure is presented.

As explained before, it is assumed that the fluorinated blocks can act as nucleating agents for the $scCO_2$ in the foaming process, due to its great $CO_2$-phicility. For this reason, a calculation of the number

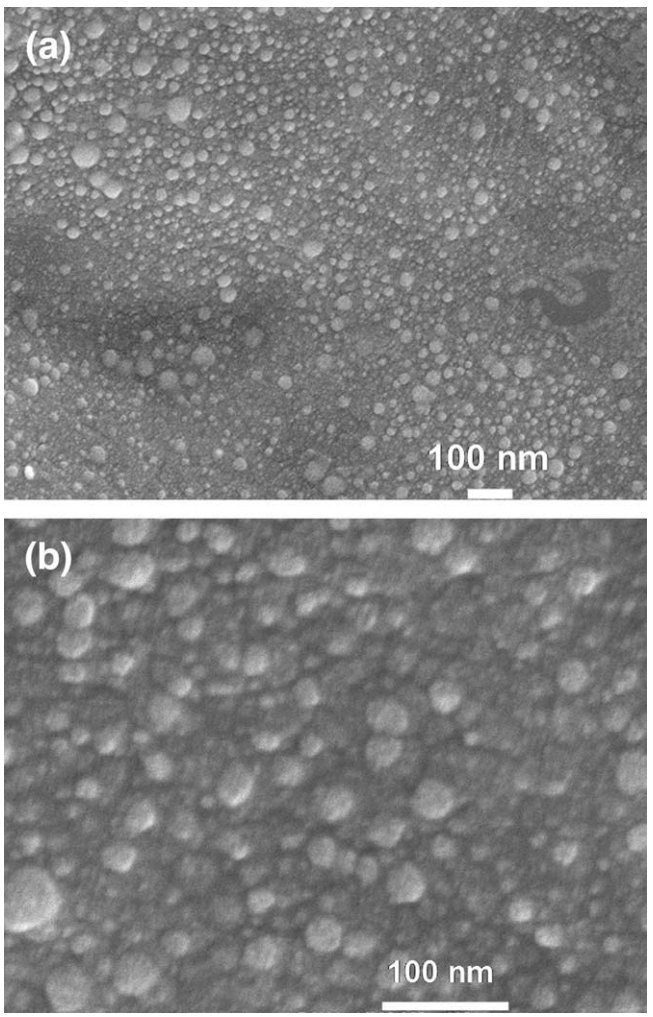


**Figure 4** SEM micrographs of PS-*b*-PFDA copolymer solid dense film (unfoamed).

of nuclei (namely $N_n$) can be performed directly from the SEM image.

Assuming an average sphere diameter ϕ of 20 nm, and taking a 3D cube of the side ($l$) of the

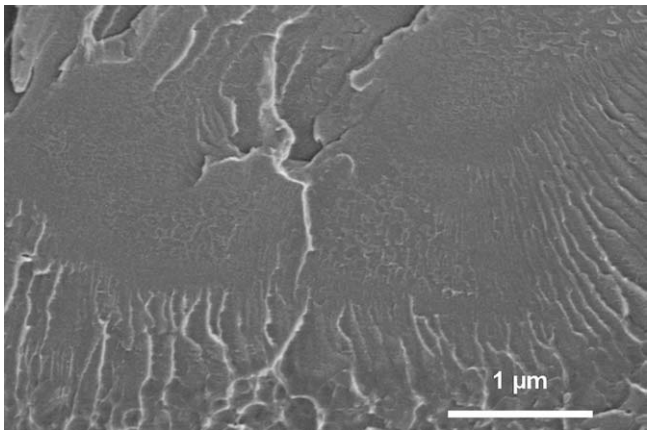


**Figure 5** SEM micrographs of the neat PS solid dense film (unfoamed).

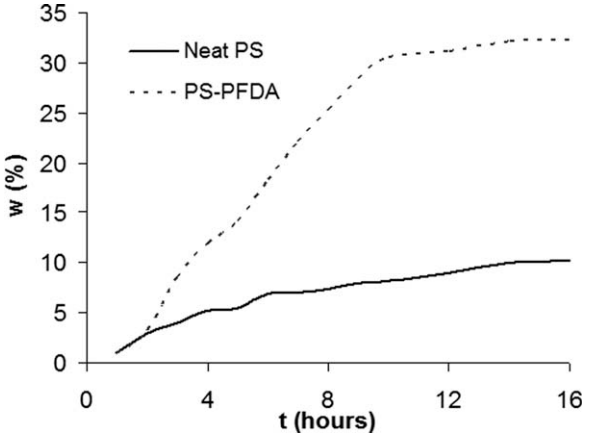


**Figure 6** Comparative $CO_2$ absorption of the bulk PS and PS-*b*-PFDA polymers (during swelling/exposure at 300 bar, 0°C).

micrograph (500 nm), the number of spheres $N_n$ inside the cube can be estimated as:

$$N_n = \left(\frac{l}{\phi}\right)^3 \quad (2a)$$

The calculation leads to a nanospheres density $N_n$ of approximately $2.25 \times 10^{17}$ spheres/cm$^3$.

This value will be compared with the cell density value obtained from eq. (1) in order to estimate an efficiency parameter which shows the number of potential nucleating agents (fluoro spheres) that lead to the cells formation during the foaming process.

### $CO_2$ absorption and foaming

The $CO_2$ affinity is measured by weighting the sample after $CO_2$ exposure at different times, up to 16 h, to determine the quantity of $CO_2$ absorbed during the saturation process. The saturation experiments were carried out at 0°C. Figure 6 presents the weight uptake of $CO_2$ in PS and PS-*b*-PFDA samples. It is clear that the PS-*b*-PFDA copolymer (40% of PFDA blocks) presents an increase of almost three times in the $CO_2$ absorption compared to neat PS (wt. of 32.2% and 8.9%, respectively). These results agree with those found in literature,[12,13,28,34] in which it is showed that solubility of fluorinated polymers is much higher than styrene-based polymers. This indicates that fluorinated blocks are acting as $CO_2$ trapping sites, leading to a great increase in the $CO_2$ solubility with respect to neat PS. To perform the supercritical foaming process, two specimens of each material were placed in the foaming reactor. The reactor was then filled with $CO_2$ at high pressure (30 MPa) and cooled down to 0°C. Saturation conditions were maintained up to equilibrium, i.e., 16 h. Then, foaming was induced by depressurization of the reactor at a constant rate of 5 MPa/min. After reaching atmospheric pressure, foamed samples were removed from the reactor to perform density measurements and cellular structure characterization.

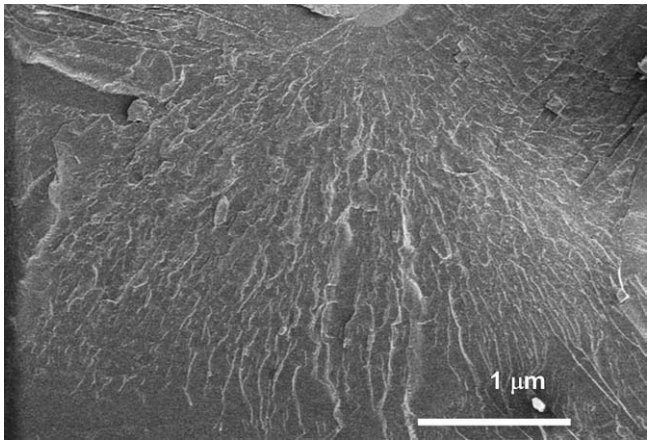


**Figure 7** SEM image of the neat PS sample after saturation in $scCO_2$ and depressurization.

SEM micrographs of neat PS foamed samples are presented in Figure 7. No cellular structure is evidenced in any of the two samples investigated. This is due to the low PS affinity for the $scCO_2$, and to the low temperatures (0°C at the beginning of the process, reaching −70°C at the end of the depressurization process, according to Fig. 1). This temperature range lies far below the depressed glass transition temperature of neat PS (about 40°C under $T_g$ obtained after saturation at 300 bar of $scCO_2$). This result has been also reported by Reglero et al.[40,41] For this reason, $scCO_2$ at low temperatures cannot lead to any cellular material in polystyrene.

A very distinct situation is exhibited when foaming the PS-*b*-PFDA samples. In Figure 8 are presented two SEM micrographs of the PS-*b*-PFDA foamed material. In this case, a quite homogenous nanocellular structure is observed, with cell sizes

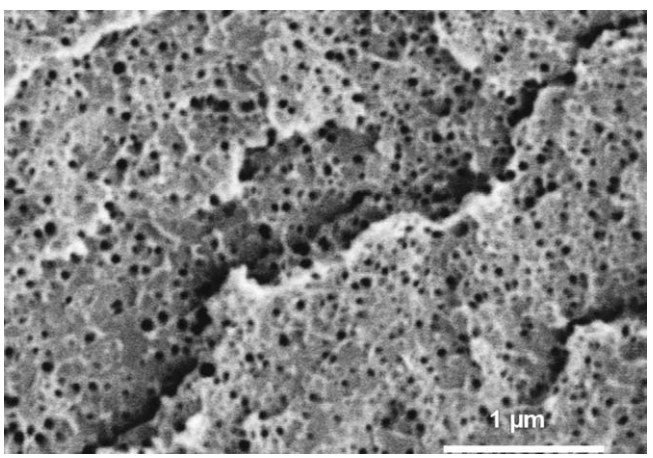


**Figure 8** SEM image of the foamed PS-*b*-PFDA blend material.

**TABLE I**
**Main Structural Characteristics of PS and PS-*b*-PFDA "Foamed" Bulk Polymers**

| Material | Relative density $\rho$ (g/cm$^3$) | Average cell size $\phi$ ($\mu$m) | Cell density $N_C$ (cells/cm$^3$) | $CO_2$ uptake (wt %) |
|---|---|---|---|---|
| PS | 0.98 | – | – | 8.9 |
| PS-*b*-PFDA | 0.70 | 0.1 | $7.3 \times 10^{14}$ | 32.2 |

between 50 nm and 100 nm. These foamed samples presented a density value of 0.7 g/cm$^3$, which indicates an expansion ratio of 1.3. For the PS-*b*-PFDA, cell formation is directly related to the high $CO_2$ affinity of the fluorinated blocks. In addition, since the glass transition temperature of fluorinated blocks is very low (−85°C from the DSC diagram showed in Fig. 3), the cell growth can occur even at low temperatures in the rubbery regime. Furthermore, growth of cells is restricted to the nanosphere radius and limited by the surrounding rigid PS blocks, which show no plasticization effect during all the process. For this reason, cell size and nanosphere radius are related for the foaming of PS-*b*-PFDA copolymer.

The cell density value $N_C$ can be related to the number of "nuclei" $N_n$ present in the solid material in the form of nano spheres. Having a look at equation 1, and taking as cell diameter $\phi$ of 50 nm, $\rho_f$ as 0.70 g/cm$^3$ and $\rho_S$ as 0.98 g/cm$^3$, the calculation of $N_c$ leads to a value of $7.3 \times 10^{14}$ cells/cm$^3$. Comparing this value to the nuclei density $N_n = 2.25 \times 10^{17}$, an efficiency factor $N_c/N_n$ value of $3 \times 10^{-2}$ is obtained. This estimated value gives an idea, of the number of nanospheres which leads to cell formation after saturation process. Thus, assuming that all the fluorinated nanospheres trap $scCO_2$, only a 3% leads to cell formation and growth, and the gas trapped in the rest of the nuclei can escape out of the sample, for example by diffusion, during the depressurization process. Moreover, a mechanism of coalescence does probably occur, although foaming at such low temperatures and using a rather low depressurization rate usually minimize this effect. Table I summarizes the main foam characteristics for the two polymers investigated.

As it has been shown, it is clear that the fluorinated blocks have a remarkable influence on the expansion process. First, they allow foaming at low temperatures because of the great difference between the $CO_2$ philicity between blocks and the depressed glass transition temperature of fluoro blocks compared with those of the PS blocks. Second, locating $CO_2$ in well-separated nanospheres assures a controlled foaming process, in which the size of the initial nucleating sites and final foam cells are correlated.

## CONCLUSIONS

Nanocellular foams with controlled cell size have been successfully obtained using a $scCO_2$ route and $CO_2$-philic block fluorinated copolymers. A simple ATRP polymerization technique was used to obtain defined fluorinated block copolymers in sufficient quantity to be used as bulk polymers or even as additives in polymer blends. A styrene-*b*-perfluorodecyl acrylate copolymer was investigated. The fluorinated blocks induce a phase separation in a polystyrene matrix in the form of nanospheres. The use of these highly $CO_2$-philic fluorinated blocks under given foaming conditions at low temperatures provides well-controlled and homogeneous nanocellular foams in copolymers, with average cell sizes below 100 nm and cell densities above $10^{14}$ cells/cm$^3$.

## References


1. Cooper, A. I. J Mater Chem 2000, 10, 207.
2. Tsivintzelis, I.; Angelopoulou, A. G.; Panayiotou, C. Polymer 2007, 48, 5928.
3. Jiang, C.; Pi, J.; Pan, Q. Polym Mater Sci Eng 2009, 25, 162.
4. Jessop, G. P.; Leitner, W. Chemical Synthesis using Supercritical Fluids: Wiley.VCH: Weinheim, 1999.
5. Baiker, A. Chem Rev 1999, 99, 453.
6. Arora, K. A.; Lesser, A. J.; McCarthy, T. J. Macromolecules 1998, 31, 2562.
7. Jacobs, L. J. M.; Danen, K. C. H.; Kemmere, M. F.; Keurentjes, T. J. F. Polymer 2007, 48, 3771.
8. Kerby, C. F.; McHugh, M. A. Chem Rev 1999, 99, 565.
9. Park, H.; Thompson, R. B.; Lanson, N.; Tzoganakis, C.; Park, C. B.; Chen, P. J Phys Chem B 2007, 111, 3859.
10. Doroudian'i, S.; Park, C. B.; Kortschot, M. Pol Eng Sci 1998, 38, 1205.
11. Xu, Z.; Jiang, X.; Liu, T.; Hu, G.; Zhao, L.; Zhu, Z.; Yuan, W. J Supercritical Fluids 2007, 41, 299.
12. Shieh, Y.; Liu, K. J Polym Res 2002, 9, 107.
13. Rindfleisch, F.; DiNoia, T. P.; McHugh, M. A. J Phys Chem 1996, 100, 15581.
14. Vitoux, P.; Tassaing, T.; Cansell, F.; Marre, S.; Aymonier, C. J Phys Chem B 2009, 113, 897.
15. O'Neill, M. L.; Cao, Q.; Fang, M.; Johnston, K. P.; Wilkinson, S. P.; Smith, C. D.; Kerschner, J. L.; Jureller, S. H. Ind Eng Chem Res 1998, 37, 3067.
16. Alessi, P.; Cortesi, A.; Kikic, I.; Vecchione, F. J Appl Polym Sci 2003, 88, 2189.
17. Chow, T. S. Macromolecules 1980, 13, 362.
18. Hwang, Y. D.; Cha, S. W. Polym Test 2001, 21, 269.
19. Yoon, J. D.; Cha, S. W. Polym Test 2001, 20, 287.
20. Hansen, N. M. L.; Jankova, K.; Hvilsted, S. Eur Polym J 2007, 43, 255.
21. Zirkel, L.; Jakob, M.; Münstedt, H. J Supercritical Fluids 2009, 49, 103.
22. Sugiyama, K.; Remoto, T.; Koide, G.; Hirao, A. Macromol Symp 2002, 181, 135.
23. Yokoyama, H.; Sugiyama, K. Macromolecules 2005, 38, 10516.
24. Li, L.; Remoto, T.; Sugiyama, K.; Yokohama, H. Macromolecules 2006, 39, 4746.
25. Di, L.; Yokohama, H.; Remoto, T.; Sugiyama, K. Adv Mater 2004, 16, 1226.

26. McHugh, M. A.; Garach-Domech, A.; Park, I. H.; Li, D.; Barbu, E.; Graham, P.; Tsibouklis, J. Macromolecules 2002, 35, 6479.
27. Renault, B.; Cloutet, E.; Lacroix-Desmazes, P.; Cramail, H. Macromol Chem Phys 2008, 209, 535.
28. André, P.; Lacroix-Desmazes, P.; Taylor, D. K.; Boutevin, B. J Supercritical Fluids 2006, 37, 263.
29. Canelas, D. A.; Bettes, De.; DeSimone, J. M. Macromolecules 1996, 29, 2818.
30. Lacroix-Desmazes, P.; André, P.; DeSimone, J. M.; Ruzette, A. V.; Boutevin, B. J Polym Sci A 2004, 42, 3537.
31. Nottelet, B.; Lacroix-Desmazes, P.; Boutevin, B. Polymer 2007, 48, 50.
32. Reglero Ruiz, J. A.; Viot, P.; Dumon, M. J Appl Polym Sci 2010, 118, 320.
33. Reglero Ruiz, J. A.; Viot, P.; Dumon, M. Cell Polym 2009, 28, 363.
34. Rindfleisch, F.; DiNoia, T. P.; McHugh, M. A. J Phys Chem 1996, 100, 15581.
35. Bouilhac, C.; Cramail, C.; Cloutet, E.; Deffieux, A.; Taton, D. J Polym Sci A 2006, 44, 6997.
36. Bouilhac, C.; Cloutet, E.; Taton, D.; Deffieux, A.; Borsali, R.; Cramail, H. J Polym Sci A 2009, 47, 197.
37. Kumar, V.; Suh, N. P. Polym Eng Sci 1990, 30, 1323.
38. Kano, Y.; Inoue, M.; Akiba, I.; Akiyama, S.; Sano, H.; Fujita, Y. J Adhesion Sci Technol 1998, 39, 6747.
39. Ren, Y.; Lodge, T. P.; Hillmyer, M. A. Macromolecules 2002, 35, 3889.
40. Reglero Ruiz, J. A.; Tallon, J.-M.; Pedros, M.; Dumon, M. J Supercritical Fluids 2011, 57, 87.
41. Reglero Ruiz, J. A.; Tallon, J.-M.; Pedros, M.; Dumon, M. J Supercritical Fluids 2011, 58, 168.